Transactions of the Nigerian Association of Mathematical Physics
Volume 4, (July, 2017), **pp273 – 280**
© Trans. of NAMP

Theoretical Study of Structural and Electronic Properties of AlAs, InAs and $Al_xIn_{1-x}As$ Alloy

[1]Nenuwe O. N. and [2]Ukhurebor E. K.*

[1]Department of Physics, Federal University of Petroleum Resources, P. M. B. 1221, Effurun, Nigeria
[2]Department of Physics, Edo University Iyamho, Edo State, Nigeria

Abstract

In this study, the atomistix toolkit-density functional theory has been used to investigate the structural and electronic properties of zinc-blende aluminum arsenide (AlAs), indium arsenide (InAs) semiconductors and aluminum indium arsenide ($Al_xIn_{1-x}As$) alloy. The generalized gradient approximation (gga) has been used to obtain the lattice parameters which are compared with both theory and experimental results. To calculate the electronic band gaps, we employed the TB09LDA meta-generalized gradient approximation (mgga), and obtained new band gaps for aluminum compositions 0.0625, 0.125, 0.1875, 0.3125, 0.3750, 0.4375, 0.5625, 0.625, 0.6875, 0.8125, 0.875 and 0.9375. It was observed that the electronic band structure of the alloys transits from direct to indirect band gap as the aluminum composition is increased from 0 to 1, which makes these new materials very interesting for applications in the fabrication of electronic, optoelectronic, photovoltaic, high-temperature and high-power electronic devices.

Keyword: Lattice parameter; Band gap; Semiconductors; Alloy.

1.0 Introduction

The group III-V semiconductors boron arsenide (BAs), aluminum arsenide (AlAs), gallium arsenide (GaAs) and indium arsenide (InAs) are very important materials in the fabrication of microwaves, optoelectronic and electronic devices. They provide a good basis for many new technological applications such as light emitting diodes, lasers, integrated circuits, modulators, photo-detectors and filters [1]. In particular, AlAs, InAs and $Al_xIn_{1-x}As$ alloy have great technological significance due to their applications in fabricating heterostructures and tuneable devices in the visible wavelength region and optoelectronic devices [2]. Aluminum arsenide is a binary semiconductor with an indirect band gap, and a zinc-blende (ZB) structure [3]. Due to its wide range applications in optoelectronics, solar cells, telecommunications, laptop computers, compact disc and telephones [4, 5], it has attracted intensive studies in recent years. Indium arsenide on the other hand is a direct band gap semiconductor with interesting applications in high-temperature and high-power electronics [6], construction of infrared detectors for wavelength range of 1-3.8μm, diode lasers, terahertz radiation source and formation of quantum dots in monolayer [7, 8]. These important physical properties can only be explained by investigating the electronic structure of these compound semiconductors and their alloys in detail. Therefore, over the years, various studies have been carried out to determine experimentally and theoretically the band structure of semiconductors including group III-V materials. For example; the band structure and density of state of XAs (X=Al, Ga, and In) have been studied by theoretical investigations [9-13]. The dielectric function corresponding to the band gap transition for AlAs has been investigated [12, 14]. Also, experimental and theoretical studies on the lattice constants have been carried out for XAs alloys [14]. Ameri et al. [15] used the Ab Initio technique to investigate the structural and electronic properties of the $Al_xIn_{1-x}As$ for x=0.25, 0.5, 0.75 and 1, and discussed the toxicology of these compounds. But the alloy was not studied for concentration x=0.0625, 0.125, 0.1875, 0.3125, 0.3750, 0.4375, 0.5625, 0.625, 0.6875, 0.8125, 0.875 and 0.9375. This alloy has distinct structural and electronic properties within these aluminum compositions that are worth investigating.

Correspondence Author: Nenuwe O.N., Email: nenuwe.nelson@fupre.edu.ng, Tel: +2348037295834

For example, Ge with indirect band gap 0.66eV is used for multijunction photovoltaic cells and Si with indirect band gap 1.12eV is also used for solar cell and photovoltaic cell fabrication [16, 17]. This alloy with band gaps 0.6692eV and 1.0938eV at compositions x=0.0625 and 0.9375 respectively, can suitably replace Ge and Si in their applications to solar and photovoltaic cells. Also, several authors [15, 18-21] have earlier reported different values of the lattice constants for AlAs and InAs.

This discrepancy has motivated us in this study to calculate the structural and electronic properties of the alloy and extend the calculations to include aluminum concentrations that have not yet been calculated before. Therefore, in this study, we present self-consistent electronic band structure calculations for AlAs, InAs semiconductors and $Al_xIn_{1-x}As$ alloy in the ZB structure using the Quantumwise ATK VNL package [8]. The Perdew-Burke Ernzerhof (PBE) exchange correlation in conjunction with the generalised gradient approximation [9-11] is used to calculate the lattice parameters for composition x(=0.000, 0.0625, 0.125, 0.1875, 0.25, 0.3125, 0.3750, 0.4375, 0.50, 0.5625, 0.625, 0.6875, 0.75, 0.8125, 0.875, 0.9375, 1.0000), and the TB09LDA [12, 13] meta-generalized gradient approximation [14, 15] is used to calculate the band gaps. The results are compared with both theoretical and experimental values available. This paper is organised as follows: Section 2 describes the computational details; the results obtained are presented in Section 3, along with discussion of correspondence between theoretical results and experimental values. Finally, the paper is concluded in Section 4.

2.0 Computational Method and Details

The density functional theory is well known for predicting too small band gaps, when calculated from the Kohn-Sham energy eigenvalues [22-30]. Nevertheless, improvements on the meta-gga functionals have allowed the calculation of accurate band gaps. Meta-generalized gradient approximation belongs to the third rung of the Jacob's ladder of exchange correlation (XC) functionals [30], as they do not only include the local density $\rho(r)$ (as in LDA; the first rung) [29] and the gradient of the density $\nabla\rho(r)$ (as in gga; the second rung), but also the kinetic-energy density [32-36]. Tran and Blaha [26] showed that accurate band gaps could be obtained for a wide range of semiconductor materials. In their calculation, the exchange potential is given by

$$v_x^{TB}(r) = c v_x^{BR}(r) + \frac{3c-2}{\pi}\sqrt{\frac{4\tau(r)}{6\rho(r)}} \quad , \quad (2.1)$$

where

$$\tau(r) = \tfrac{1}{2}\sum_{i=1}^{N}\left|\nabla\psi_i(r)\right|^2 \quad , \quad (2.2)$$

is the kinetic-energy density, $\psi_i(r)$ is the ith Kohn-Sham orbital, and $v_x^{BR}(r)$ is the Becke-Roussel exchange potential [36]. The c-parameter is calculated as

$$c = \alpha + \beta\left(\frac{1}{\Omega}\int_{\Omega}\frac{\left|\nabla\rho(r)\right|}{\rho(r)}dr\right)^{\frac{1}{2}} \quad , \quad (2.3)$$

where $\alpha = 0.012$ and $\beta = 1.023\ \mathrm{Bohr}^{\frac{1}{2}}$ are determined by fitting to reproduce the experimental band gaps of a large number of semiconductors and insulators and Ω is the volume of the cell. The correlation potential used by Tran and Blaha is an ordinary LDA correlation. In the atomistix toolkit (ATK) one can actually use the XC functional by Tran and Blaha in two ways: (i) specify the XC functional as exchange_correlation = MGGA.TB09LDA, in which case the c-parameter is determined self-consistently based on the expression Eqn. (2.3), and (ii) set the value of the c-parameter manually as exchange_correlation = MGGA.TB09LDA(c=1.0). Here, the electron and kinetic-energy densities are still calculated self-consistently, but using the fixed value of c. We must note that a self-consistent determination of the c-parameter should only be done for a bulk configuration that is periodic in all directions, otherwise it gives diverging results.

In this study, we calculate the structural and electronic properties of AlAs, InAs and $Al_xIn_{1-x}As$ alloy using the atomistix toolkit-density functional theory code from Quantumwise [22, 37] implemented in virtual nanolab (VNL) 2016.2 [37-39]. The exchange correlation effects were treated using the gga and mgga [23-25, 28, 29] with virtual crystal approximation (VCA) [40-43]. The numerical accuracy is determined with a density mesh cut-off 300 Hartree at room temperature (300K), and numerical iteration of Brillouin zone was performed using a k-mesh of dimension 256 symmetry k-points in the Monkhorst-pack grid [44]. The generalized gradient approximation was used to calculate the lattice parameters of $Al_xIn_{1-x}As$ for composition varying from $0 \le x \le 1$ in steps of 0.0625.

The composition x=0 and 1 gives the binary semiconductors InAs and AlAs respectively. The virtual crystal approximation with the OMX pseudopotential and basis set tier 3 were also used to calculate the lattice constants in the whole composition region. For the gga calculations we set the exchange functional to PBE [45]. It is well known [22] that OMX pseudopotentials have more valence electrons in the cores. This prompted the use of good basis set and high-density mesh cut-off energy of 300 Hartree. The virtual crystal basis is constructed with a number $0 \leq x \leq 1$, defining the fraction of the first basis set corresponding to the $Al_xIn_{1-x}As$ mixture. It is then associated with atoms in the configuration corresponding to the first element aluminum in the list. The total energy is then calculated for the AlAs lattice constant and the aluminum percentage x specified in $Al_xIn_{1-x}As$. In order to determine the equilibrium parameter for a given composition x(=0.000, 0.0625, 0.125, 0.1875, 0.25, 0.3125, 0.3750, 0.4375, 0.50, 0.5625, 0.625, 0.6875, 0.75, 0.8125, 0.875, 0.9375, 1.0000), we calculate the total energy for a range of lattice constants and obtain the one with the lowest energy. When the calculation is done, a python script is used to virtualize and analyse the result. All the total energy objects of each x value are read, and a fit is performed close to the minimum energy in order to find the equilibrium lattice parameter. Thereafter, the lattice parameter obtained is plotted against the composition x, as displayed in Figure 1.

Calculations of the band gap for each aluminum composition were performed within the meta-generalized gradient approximation for the TB09LDA exchange correlation functional using the lattice parameters obtained above. The self-consistent calculations were made with tolerance $1.0e^{-4}$ Hartree, maximum steps 100, damping factor 0.1, history steps 20, mixing variable as Hamiltonian variable and c-parameter as 0.98. Integration over the irreducible Brillouin zone was performed up to 256 k-points (8X8X8 meshes) for AlAs, InAs and $Al_xIn_{1-x}As$. The Hartwigsen-Goedecker-Hutter (HGH) pseudopotentials [46]: HGH[Z=3]LDA.PZ, HGH[Z=13]LDA.PZ and HGH[Z=5]LDA.PZ for Al, In and As, with basis set tier3 each were used for the calculation. The Brillouin zone and points per segment were set to G, X, W, L, G, K, X, U, W, K, L and 100 respectively. The process is programmed by looping over x-values and using the equilibrium lattice parameters already obtained to calculated the band structure. At the end of the calculations the energy band gaps are extracted and plotted against the composition x, as displayed in Table 3 and Figure 2.

3.0 Results and Discussion

3.1 Structural Properties

The structural properties of AlAs, InAs semiconductor and their alloy $Al_xIn_{1-x}As$ are calculated using gga and PBE exchange-correlation functional. The structural optimization was performed by starting from an experimental value with respect to the cell parameters and also the atomic positions for the ternary material $Al_xIn_{1-x}As$ with different Al composition x. At each composition, the optimized equilibrium lattice parameters, with experimental and theoretical results are displayed in Table 1.

Table 1. Lattice parameters obtained with gga for AlAs, InAs and $Al_xIn_{1-x}As$ compared to other theoretical calculations and experimental data

$a(\dot{A})$			
Compound	Current work	Theoretical calculations	Experimental data
InAs	6.0042	6.077[(a)], 6.239[(a)], 5.921[(b)], 5.902[(c)], 6.030[(d)]	6.036[(e)]
$Al_{0.0625}In_{0.9375}As$	5.6759	-	-
$Al_{0.1250}In_{0.8750}As$	5.6786	-	-
$Al_{0.1875}In_{0.8125}As$	5.6797	-	-
$Al_{0.2500}In_{0.7500}As$	5.6818	5.978[(a)], 5.978[(a)]	-
$Al_{0.3125}In_{0.6875}As$	5.6829	-	-
$Al_{0.3750}In_{0.6250}As$	5.6838	-	-
$Al_{0.4375}In_{0.5625}As$	5.6845	-	-
$Al_{0.5000}In_{0.5000}As$	5.6856	5.871[(a)], 6.009[(a)]	-
$Al_{0.5625}In_{0.4375}As$	5.6864	-	-
$Al_{0.6250}In_{0.3750}As$	5.6872	-	-
$Al_{0.6875}In_{0.3125}As$	5.6884	-	-
$Al_{0.7500}In_{0.2500}As$	5.6891	5.765[(a)], 5.878[(a)]	-
$Al_{0.8125}In_{0.1875}As$	5.6904	-	-
$Al_{0.8750}In_{0.1250}As$	5.6909	-	-
$Al_{0.9375}In_{0.0625}As$	5.6915	-	-
AlAs	5.6920	5.639[(a)], 5.742[(a)], 5.633[(d)], 5.734[(d)], 5.644[(f)]	5.661[(g, h)]

[a]Ref.[21], [b]Ref.[15], [c]Ref.[19], [d]Ref.[20], [e]Ref.[47], [f]Ref.[18], [g]Ref.[48], [h]Ref.[49]

The calculated value for AlAs and InAs are in excellent agreement with experiment and theoretical studies which is due to the fact that gga yields parameters which are in between the overestimated and underestimated results of market standard [49, 50] gga functional. The lattice constant calculated for AlAs overestimated the experimental value 5.661Å by 0.54% and the gga value for InAs underestimated the experimental value 6.036Å by 0.53%.

The behaviour of the lattice parameters of ternary mixed crystal with composition x, can be expressed as a linear combination of the lattice parameter of the two constituent binary alloys according to Vegard's law [51, 52]

$$a_{\mathrm{Al_xIn_{1-x}As}} = x.a_{\mathrm{AlAs}} + (1-x)a_{\mathrm{InAs}} \tag{3.1}$$

Where, a_{AlAs}, a_{InAs} and $a_{\mathrm{Al_xIn_{1-x}As}}$, are respectively, the lattice parameters of the materials AlAs, InAs and $Al_xIn_{1-x}As$. Table 2 shows Vegard's predictions for the lattice parameters while, Figure 1 displays the comparison between results obtained for the calculated lattice constants and those obtained from Vegard's law [51, 52] for the alloy $Al_xIn_{1-x}As$ at different composition x. It is clear from Figure 1 that the lattice constant of $Al_xIn_{1-x}As$ varies with change in Al composition. To the best of our knowledge, there are no experimental values for the structural properties of the ternary mixed crystal $Al_xIn_{1-x}As$. Our results for x = 0.25, 0.5 and 0.75 are smaller than results obtained by Ameri et al. [19]. The results for 0.0625, 0.125, 0.1875, 0.3125, 0.375, 0.4375, 0.5625, 0.6250, 0.6875, 0.8125, 0.875 and 0.9375 are quite new in the literature. It is important to state that increase in Al composition from 0 to 0.0625 leads to a decrease in lattice constant as shown in Figure 1. Usually, a decrease in lattice constant is accompanied by corresponding increase of the bulk modulus [19]. This represents bond strengthening or weakening effect induced by changing the concentration.

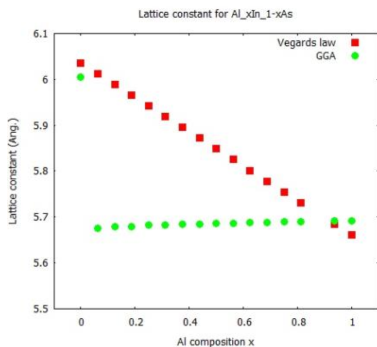

Figure 1. Concentration dependence of the computed lattice constants using gga for $Al_xIn_{1-x}As$ alloy compared with Vegard's prediction.

Table 2. Lattice parameter predictions from Vegard's law for $Al_xIn_{1-x}As$ alloy

$a(\dot{A})$

Compound	Predictions from Vegard's law
$Al_{0.0625}In_{0.9375}As$	6.0125
$Al_{0.1250}In_{0.8750}As$	5.9891
$Al_{0.1875}In_{0.8125}As$	5.9656
$Al_{0.2500}In_{0.7500}As$	5.9422
$Al_{0.3125}In_{0.6875}As$	5.9188
$Al_{0.3750}In_{0.6250}As$	5.8953
$Al_{0.4375}In_{0.5625}As$	5.8719
$Al_{0.5000}In_{0.5000}As$	5.8485
$Al_{0.5625}In_{0.4375}As$	5.8250
$Al_{0.6250}In_{0.3750}As$	5.8016
$Al_{0.6875}In_{0.3125}As$	5.7781
$Al_{0.7500}In_{0.2500}As$	5.7547
$Al_{0.8125}In_{0.1875}As$	5.7313
$Al_{0.8750}In_{0.1250}As$	5.7978
$Al_{0.9375}In_{0.0625}As$	5.6844

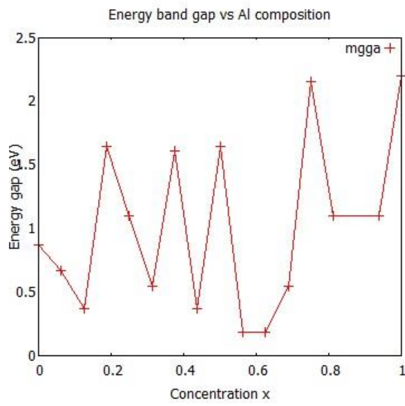

Figure 2. Concentration dependence of the band gap within mgga for $Al_xIn_{1-x}As$ alloy.

3.2 Electronic Properties

The wide range application of semiconductors and their alloys in specific electronic devices calls for a comprehensive understanding of the energy band gaps. On this study, the electronic band structures of AlAs, InAs and $Al_xIn_{1-x}As$ alloy were calculated using mgga and TB09LDA exchange correlation functional for the entire region of Al composition $0 \leq x \leq 1$. This method uses the Hartwigsen-Goedecker-Hutter (HGH) pseudopotentials [53-55] and tier three basis set. The electronic band structure was calculated for these materials using the equilibrium lattice parameters obtained from the gga. The electronic band structures obtained by the use mgga for InAs, $Al_{0.375}In_{0.625}As$, $Al_{0.75}In_{0.25}As$, $Al_{0.8125}In_{0.1875}As$, $Al_{0.875}In_{0.125}As$ and AlAs are displayed in Figures 3 – 8. It is clear that the band gap in InAs is a direct band gap due to the fact that both the valence band maximum and conduction band minimum are located at the gamma (G) point, while in AlAs is an indirect band gap since the valence band maximum is located at point G and the conduction band minimum is located at point X in accordance with the existing literature data. The other alloys possess direct band gap. Therefore, we can conclude that the electronic band structure of the $Al_xIn_{1-x}As$ material transit from direct to indirect band gap when doping aluminum atoms in InAs crystal. Due to the fact that phonon participates in inter-band transitions, it also makes this indirect band gap materials suitable for optoelectronic and photovoltaic devices.

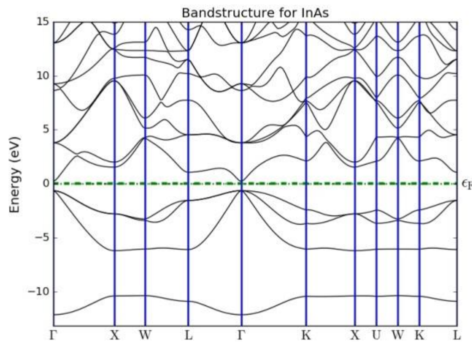

Figure 3. Band structure of InAs.

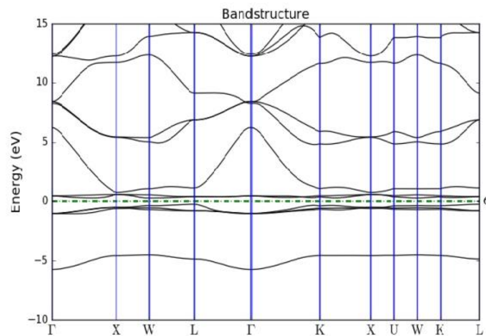

Figure 4. Band structure of $Al_{0.375}In_{0.625}As$ alloy.

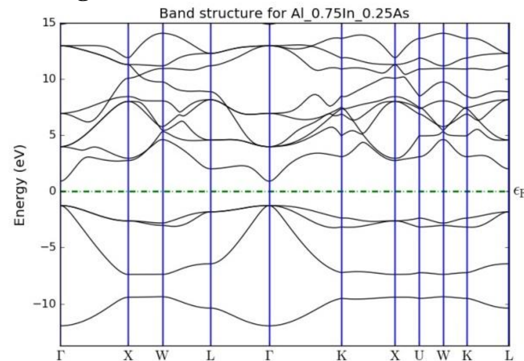

Figure 5. Band structure of $Al_{0.75}In_{0.25}As$ alloy.

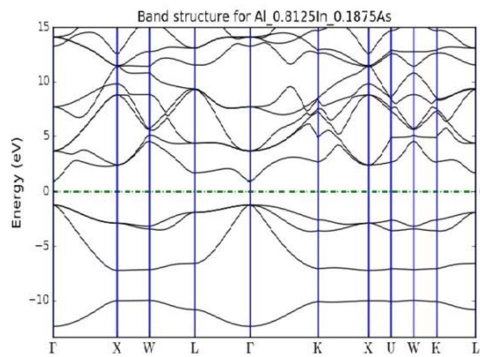

Figure 6. Band structure of $Al_{0.8125}In_{0.1875}As$ alloy.

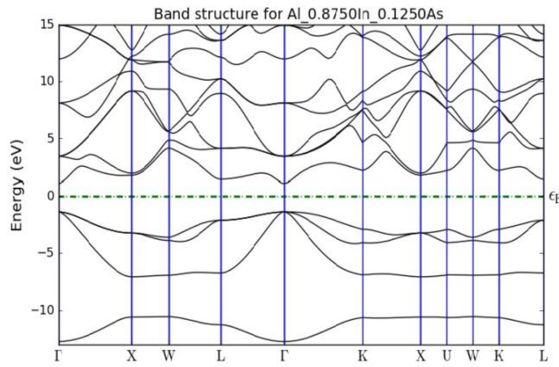

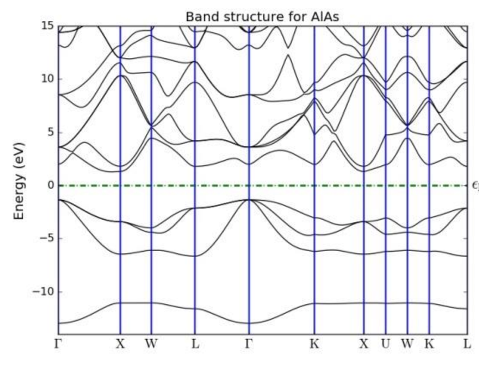

Figure 7. Band structure of $Al_{0.875}In_{0.125}As$ alloy. **Figure 8. Band structure of AlAs.**

Table 3. Band gap calculated with MGGA for AlAs, InAs and $Al_xIn_{1-x}As$ compared to other theoretical calculations and experimental data

E_g (eV)			
Material	Current work	Theoretical calculations	Experimental data
InAs	0.8720	1.68[(a)]	0.420[(b)]
$Al_{0.0625}In_{0.9375}As$	0.6692	-	
$Al_{0.1250}In_{0.8750}As$	0.3645	-	
$Al_{0.1875}In_{0.8125}As$	1.6406	-	
$Al_{0.2500}In_{0.7500}As$	1.0937	0.939[(a)]	
$Al_{0.3125}In_{0.6875}As$	0.5468	-	
$Al_{0.3750}In_{0.6250}As$	1.6050	-	
$Al_{0.4375}In_{0.5625}As$	0.3645	-	
$Al_{0.5000}In_{0.5000}As$	1.6406	1.200[(a)]	
$Al_{0.5625}In_{0.4375}As$	0.1820	-	
$Al_{0.6250}In_{0.3750}As$	0.1822	-	
$Al_{0.6875}In_{0.3125}As$	0.5468	-	
$Al_{0.7500}In_{0.2500}As$	2.1500	1.540[(a)]	
$Al_{0.8125}In_{0.1875}As$	1.0937	-	
$Al_{0.8750}In_{0.1250}As$	2.5520	-	
$Al_{0.9375}In_{0.0625}As$	1.0938	-	
AlAs	2.201	1.360[(a)]	2.22[(c)]

[a]Ref.[15], [b]Ref.[48], [c]Ref.[46]

The calculated results for energy band gaps are displayed in Table 3 and compared with different theoretical results and experimental values available. The band gap 0.892eV obtained for InAs overestimated the experimental value 0.42eV [48]. This trend has been earlier observed by Ameri et al. [15]. But, the calculated energy band gap of 2.201eV for AlAs underestimated the experimental value. Figure 2 indicates the band gap as a function of Al composition x, using meta-generalised gradient approximation. It is clear that the band gap is sensitive to the Al composition x. This implies that the band gap exhibits strong composition dependence. New band gaps are obtained for the Al compositions 0.0625, 0.125, 0.1875, 0.3125, 0.3750, 0.4375, 0.5625, 0.625, 0.6875, 0.8125, 0.875 and 0.9375. It was observed that the electronic band structure of the alloys transits from direct to indirect band gap as the aluminum composition is increased from 0 to 1. It is very important to note that the band gap of the ternary alloy $Al_xIn_{1-x}As$, 0.6692eV and 1.0938eV obtained at compositions x=0.0625 and 0.9375 can suitably replace Ge and Si in their applications to solar and photovoltaic cells, due to the fact that Ge with indirect band gap 0.66eV is used for multijunction photovoltaic cells and Si with indirect band gap 1.12eV is also used for solar cell and photovoltaic cell fabrication [16, 17]. This makes these new materials very interesting for applications in the fabrication of electronic, optoelectronic, photovoltaic, high-temperature and high-power electronic devices.

4.0 Conclusion

The use of ATK-DFT implemented in virtual nanolab 2016.2, enabled us to evaluate the structural and electronic properties of the binary semiconductors AlAs and InAs, and their alloy $Al_xIn_{1-x}As$ within the composition range $0 \leq x \leq 1$. We also calculated the variation in lattice constants and band gap with respect to the doping compositions x. It was observed that the composition dependent lattice parameter deviates from Vegard's law. This deviation might be as a result of the binary compounds AlAs and InAs having unequal lattice parameters.

The electronic band structure of this alloy transits from direct to indirect band gap when doping aluminum atoms in InAs crystal. These new materials with aluminum composition x=0.0625, 0.125, 0.1875, 0.3125, 0.3750, 0.4375, 0.5625, 0.625, 0.6875, 0.8125, 0.875 and 0.9375 are exciting and will find useful applications in the fabrication of electronic, optoelectronic, photovoltaic, high-temperature and high-power electronic devices.

References

[1] Vurgaftman, I. and Meyer, J.R. (2003). Band Gap for III-V Semiconductors, *Journal of Applied Physics*, **94**(6), 3675-3696.

[2] Gupta, D.C. and Kulshrestha, S. (2009). Effect of High Pressure on Polymorphic Phase Transition and Electronic Structure of XAs (X = Al, Ga, In), *Phase Transitions*: *A Multinational Journal*, **82**(12), 850-865.

[3] Grundmann, M. (2010). The Physics of Semiconductors, Spring-Verlag Berlin Heidelberg, 2nd Edn.

[4] Mohammad, R. (2005). The Band Structure of III (In, Al, Ga) –V (N, As, Sb) Compounds and Ternary Alloys, M.Sc. Thesis, Middle East Technical University, 1-179.

[5] Isa, H.I. and Abdul-Lettif, A.M. (2012). Electronic Structure of AlAs Nanocrystals, *American J. Conds. Matt. Phys*., **2** (4), 83-87.

[6] Arabshahi, H., Khalvati, M. R., & Rokn-Abadi, M. R. (2008). Temperature and Doping Dependencies of Electron Mobility in InAs, AlAs and AlGaAs at High Electric Field Application. *Brazilian Journal of Physics*, **38**(3A), 293-296.

[7] Lide, D.R. (1998). Hand Book of Chemistry and Physics (87 Edn.), Boca Raton, FL: CRC Press, 4-61.

[8] Azo Materials, www.azom.com.

[9] Srivastava, A., Tyagi, N. Sharma, U.S. and Singh, R.K. (2011). Pressure Induced Phase Transformation and Electronic Properties of AlAs, *Materials Chemistry and Physics*, **125**(1-2), 66-71.

[10] Aourag, H., Ferhat, M., Bouhafs, B., Bouarissa, N., Zaoui, A., Amrane, N. and Khelifa, B. (1995). Band Structure Calculations of Ga1−*x*Al*x*As, GaAs1−*x*P*x* and AlAs under Pressure, *Computational Materials Science*, **3**(3), 393-401.

[11] Aouina, N.Y., Mezrag, F., Boucenna, M., El-Farra, M. and Bouarissa, N. (2005). High Pressure Electronic Properties and Elastic Stability Criteria of AlAs, *Materials Science and Engineering*: *B*, **123**(1), 87-93.

[12] Johnson, K.A. and Ashcroft, N.W. (1998). Correction to Density Functional Theory Band Gap, *Physical Review B*, **58** (23), 15548-15556.

[13] Amrani, B. (2006). First Principles Investigation of AlAs at High Pressure, *Superlattices and Microstructures*, **40**(2), 65-76.

[14] Reshak, A.H. and Auluck, S. (2007). Investigation of the Electronic Properties, First and Second Harmonic Generation for AXIIIBXV Zinc-Blende Semiconductors, *Physica B*: *Condensed Matter*, **395**(1-2), 143-150.

[15] Ameri, M., Boufadi, F., Touia, A., Faudil, M., Hachemane, D., Boudia, K., Slamani, A. and Aze-Eddine,A. (2012).Ab Initio Calculations Study of Structural and Electronic Properties of Ternary Alloy AlxIn1–xAs, Materials Sciences and Applications, 3(10), 674-683.

[16] Stephen T.T. and Andrew, R. (2006). Modern Physics: for Scientists and Engineers, Third Edition, Thomson: Brooks/Cole, Australia, 392-402.

[17] Cowand, J.A. and O'Dell, A. (1996). Band gap energy measurements for silicon and germanium diodes, *http://webphysics.davidson.edu/alumni/jocowan/Abstract.htm*.

[18] Wang, S. Q., & Ye, H. Q. (2002). A Plane-wave Pseudopotential Study on III–V Zinc-Blende and Wurtzite Semiconductors under Pressure, *Journal of Physics: Condensed Matter*, 14(41), 9579.

[19] Van Camp, P. E., Van Doren, V. E., & Devreese, J. T. (1990). Pressure Dependence of the Electronic Properties of cubic III-V In compounds. *Physical Review* B, **41**(3), 1598.

[20] Ahmed, R., Hashemifar, S. J., Akbarzadeh, H., & Ahmed, M. (2007). Ab initio Study of Structural and Electronic Properties of III-arsenide Binary Compounds. *Computational materials science*, **39**(3), 580-586.

[21] Adachi, S. (2005). Optical Properies, in Properties of Group-IV, III-V and II-VI Semiconductors, **John Wiley & Sons**, Ltd, Chichester, **UK**. doi:10.1002/0470090340-ch3.

[22] Atomistix ToolKit 2016.2, Quantum Wise A/S, www.quantumwise.com

[23] Perdew, J.P., Burke, K. and Ernzerhof, M. (1996). Generalized Gradient Approximations made Easy, *Phys. Rev. Lett.***77**(18), 3865.

[24] Engel, E. and Vosko, S. H. (1993). Exact Exchange-only Potentials and the Virial relation as Microscopic Criteria for Generalized Gradient Approximations, *Phys. Rev*. B **47**, 13164.

[25] Perdew, J.P. and Yue, W. (1992). Accurate and Simple Analytic Representation of the Electron-Gas Correlation Energy, *Phys. Rev*. B **45**, 13244.

[26] Tran, F. and Blaha, P. (2009). Accurate Band Gaps of Semiconductors and Insulators with a Semilocal Exchange-Correlation Potential, *Phys. Rev. Lett*. **102**, 226401.

[27] Kim, Y.S., Marsman, M., Kresse, G., Tran, F. and Blaha, P. (2010). Towards Efficient Band Structure and Effective Mass Calculations for III-V Direct Band-gap Semiconductors", *Phys. Rev*. B **82**(20), 205212.

[28] Perdew, J. P., Tao, J., Staroverov, V. N., & Scuseria, G. E. (2004). Meta-Generalized Gradient Approximation: Explanation of a realistic Non-Empirical Density Functional. *J. Chem. Phys*.,**120**(15), 6898-6911.

[29] Sun, J., Marsman, M., Csonka, G. I., Ruzsinszky, A., Hao, P., Kim, Y. S., and Perdew, J. P. (2011). Self-consistent Meta-Generalized Gradient Approximation within the Projector-Augmented-Wave Method. *Phys. Rev*. B, **84**(3), 035117.

[30] Perdew, J.P. and Schmidt K. (2001), Density Functional Theory and Its Applications to Materials, edited by V. E. van Doren, C. van Alsenoy, and P. Geerlings (American Institute of Physics, Melville).

[31] Kohn, W., & Sham, L. J. (1965). Self-Consistent Equations including Exchange and Correlation Effects, Phys. Rev., 140(4A), A1133.

[32] Perdew, J.P., Burke, K. and Ernzerhof M. (1996). Generalized Gradient Approximation Made Simple, Phys. Rev. Lett., 77(18), 3865-3868.

[33] Engel, E. and Vosko, S.H. (1994). Fourth-order Gradient Corrections to the Exchange-only Energy Functional: Importance of ∇2n Contributions, Phys. Rev. B 50, 10498.

[34] Michael, F. and Walter, T. (1998). Exchange-correlation Density Functional beyond the Gradient Approximation, Phys. Rev. A 57, 189

[35] Perdew, J.P., Ruzsinszky, A. Csonka, G.I. Constantin, L.A. and Sun, J. (2009). Workhorse Semilocal Density Functional for Condensed Matter Physics and Quantum Chemistry Phys. Rev. Lett. 103, 026403.

[36] Becke, A. D., and Roussel, M. R. (1989). Exchange holes in inhomogeneous systems: A coordinate-space model. Physical Review A, 39(8), 3761.

[37] Brandbyge, M., Mozos, J. L., Ordejón, P., Taylor, J., & Stokbro, K. (2002). Density-Functional Method for Nonequilibrium Electron Transport, Phys. Rev. B **65**(16), 165401.

[38] Seid, A., Go¨rling, A., Vog, P. and Majewski, J. A. (1996). Generalized Kohn-Sham Schemes and the Band Gap Problem, *Phys. Rev*. B **53**(7), 3764-3774.

[39] Castro, A., Marques, M. A., and Rubio, A. (2004). Propagators for the Time-Dependent Kohn–Sham Equations. *Journal of Chemical Physics*, **121**(8), 3425-3433.

[40] Elabsy A.M. and Elkenany E.B. (2010). Thermal Response to Electronic Structures of Bulk Semiconductors, *Physica* B: Condensed Matter, **405** (1), 266-271.

[41] Elabsy A.M., Degheidy A.R., Abdelwahed H.G. and Elkenany E.B. (2010). Pressure Response to Electronic Structures of Bulk Semiconductors at room Temperature, *Physica* B: Condensed Matter, **405** (17), 3709-3713.

[42] Degheidy, A.R. and Elkenany, E.B. (2011). Effect of Pressure and Temperature on Electronic Structure of GaN in the zinc blende Structure, *Semiconductors***45**, 1251.

[43] Nadir B. and Mustapha B., (2008). Band Parameters for AlAs, InAs and their Ternary Mixed Crystals, *Physica Scripta*, **79**, (1),015701.

[44] Hendrik, J.M. and James, D.P (1976). Special Points for Brillouin-zone Integrations, *Phys. Rev*. B **13**, 5188.

[45] Perdew, J.P. and Zunger, A. (1981). Self-interaction Correction to Density-functional Approximations for Many-electron Systems, *Phys. Rev*. B **23**, 5048.

[46] Krack, M. (2005). Pseudopotentials for H to Kr Optimized for Gradient-Corrected Exchange-Correlation Functionals. *Theoretical Chemistry Accounts: Theory, Computation, and Modeling (Theoretica Chimica Acta)*, **114**(1), 145-152.

[47] Wyckoff, R.W.G. (1986). Crystal Structures, 2nd Edition, Krieger, Malabar.

[48] Vurgaftman, I., Meyer, J.R. and Ram-Mohan, L.R. (2001). Band Parameters for III-V Compound Semiconductors and their Alloys, *J. Appl. Phys*. **89**, 5815.

[49] Brikia, M., Abdelouhaba, M., Zaouib, A. and Ferhata, M. (2009). Relativistic Effects on the Structural and Transport Properties of III–V Compounds: A First-Principles Study, *Superlattice and Microst*. **45**(2), 80–90.

[50] Noor, N.A., Ali, S., Murtaza, G., Sajjid, M., Alay-e-Abba, S.M., Shaukat, A., Alahmed, Z.A. and Reshak, A.H. (2014). Theoretical Investigation of Band Gap and Optical Properties of $ZnO_{1-x}Te_x$ Alloy (x = 0, 0.25, 0.5, 0.75 and 1), Computational Material Science, **93**, 151-159.

[51] Vegard, L.Z. (1921). Formation of Mixed Crystals by Solid- Phase Contact, *Journal of Physics*, **5**(5), pp. 393-395.

[52] Denton, R.A. and Ashcnoft, N.W. (1991). Vegard's Law, *Physical Review A*, **43**(6),3161-3164.

[53] Hartwigsen, C., Gœdecker, S., & Hutter, J. (1998). Relativistic separable dual-space Gaussian pseudopotentials from H to Rn. Physical Review B, **58**(7), 3641.

[54] Willand, A., Kvashnin, Y.O., Genovese, L., Vázquez-Mayagoitia, A., Deb, A.K., Sadeghi, A., Deutsch, T. and Goedecker, S. (2013). Norm-Conserving Pseudopotentials with Chemical Accuracy Compared to All-electron Calculations, *Journal of Chemical Physics***138**, 104109.

[55] Brikia, M., Abdelouhaba, M., Zaouib, A. and Ferhata, M. (2009). Relativistic Effects on the Structural and Transport Properties of III–V Compounds: A First-Principles Study, *Superlattice and Microst*. **45**(2), 80–90.